ENERGY, EXERGY AND EMISSION ANALYSIS OF PROPOSED BRAYTON-BRAYTON HYBRID CYCLE FOR AUXILIARY POWER UNIT IN AIRCRAFT SYSTEM

Anupam Kumari
Assistant Professor
Department of Mechanical Engineering
ARKA JAIN University Jharkhand,India
Email: dr.anupam@arkajainuniersity.ac.in

Abstract : The present work details thermodynamic and emission analysis of a Brayton-Brayton hybrid gas turbine cycle for Auxiliary Power Unit (APU) in aircraft applications. Energy, exergy and emission analysis of the proposed brayton -brayton cycle has been considered in order to establish its importance in futuristic auxiliary power units in aviation sector. The analyzed cycle comprises of two-gas turbine cycles back to back with one acting as the higher temperature topping cycle and the other utilizing the heat of the topping cycle and acting as the lower temperature bottoming cycle. Component level thermodynamic mathematical modeling of components of brayton-brayton cycle has been done. A code has been developed in C++ programming language which is based on the thermodynamic model of cycle components proposed. Results show that, the specific work initially increases with increase of pressure ratio ($r_{p,c}$) at any turbine inlet temperature (TIT) but it starts decreasing at very high values of $r_{p,c}$. Gas turbine efficiency and specific work both increase for a fixed value of $r_{p,c}$ with the increase in TIT. The cycle is best suited for applications where power requirement ranges between 300-550 kJ/kg. The exergy analysis shows that maximum exergy loss of around 27% occurs during combustion in the cycle. The emission analysis shows that with increase in compressor pressure ratio NO_X and primary-zone-temperature increase whereas CO and UHC emission decreases.

Keywords: Brayton-brayton cycle; emission; equivalence ratio; exergy; exergy loss; hybrid cycle.

Nomenclature

c_p = specific heat…………..(kJ-kg^{-1}·K^{-1})

gt = gas turbine

h = specific enthalpy………(kJ·kg^{-1})

ΔH_r = lower heating value……(kJ.kg^{-1}K^{-1})

$\dot{m}$ = mass flow rate……….. (kg·s^{-1})

Q = heat added/ removed during process

r_p = cycle pressure ratio

p = pressure………………..(bar)

T = temperature……………(K)

TIT = turbine inlet temperature (K)

W = specific work………(kJ·kg^{-1})

Gr = Gibbs free energy function =43890 kJ/kg

I. INTRODUCTION

The aircraft industries have been trying hard to opt for a concept of More Electric Aircraft aiming at conventional systems in the aircrafts to be replaced by the electrical counterparts [1-2]. The replacement has resulted in terms of increased efficiency compared to the existing one's. The study reveals that air passenger traffic is increasing annually at a rapid pace of 5%. The traffic growth and unparalleled jams have resulted in harmful emissions like NOx, CO and UHCs [3-4]. According to researchers, the pace at which the global air pollution is increasing; it might result in subsequent aviation emissions, if more efficient cycles would not be adopted. Also, search of leaner and cleaner air travel has led to an increase in the search of more efficient technologies and hence several attempts have been made to implement the same. One of those systems is Auxiliary Power Unit (APU) that consist of a gas turbine which is utilized for taking care of cabin cooling, lighting, starting the main engines and providing power for aircraft controls. APU systems are generally placed in the tails of larger jets and turboprop engines and these are used to provide auxiliary power for running above discussed applications when main engines are shut off and no other electrical supply is there. Many aircrafts APUs are also operated in-flight which provides backup power for the main engines. Traditional APUs have very low efficiencies and in order to increase the efficiency a hybrid cycle has been proposed here. Also, APU systems are responsible for ground level pollution especially NOx, which is responsible for acid rain as well. In the last few decades several attempts have been made integrating the APU with different cycles. The present paper represents a proposed APU cycle which incorporates a Brayton-Brayton cycle instead of conventional APU system. The proposed cycle is predicted to have an upper hand in terms of efficiency and reducing emissions. The present cycle further includes air-film blade cooling technique as the gas turbine blade cooling technique.

Several research articles are available related to conventional APU and air-film blade cooling techniques.

Air film blade cooling technique is most promising turbine blade cooling technique and several research papers have been published incorporating this. Sanjay et al. [5] investigated thermodynamic performance of combine cycle using air-film blade [AFC] cooling technique. Sanjay [6] carried out component-wise exergy analysis of gas-steam combined cycle using AFC technique. Kumari and Sanjay [7] calculated the 3-E (Energy, Exergy and Emission) performance analysis of gas turbine cycle adopting AFC as blade cooling technique. Mishra and Sanjay [8] investigated energy and exergy based performance of gas turbine cycle adopting AFC and predicted the thermal performance in terms of efficiency and specific work output. Shukla and Singh [9] predicted the thermodynamic performance of steam injected gas turbine based power cycle adopting air film blade cooling technique. Mishra et al. [10] carried out advanced exergy analysis of air-film blade cooled marine gas turbine (LM-2500+) and found out that endogenous exergy destruction was found to be superior over exogenous destruction. The author also concluded that combustor is the main source of exergy destruction. Choudhary et al. [11] proposed SOFC-APU hybrid system for aircraft power generation. The authors investigated the proposed system on the ground of first and second law and predicted that efficiency can be increased upto ~ 62%. Few articles [12-13] have also been found which directly investigates about replacing the existing conventional APUs. Rajashekara et al. [14] carried out simulation of 440 kW APU system weighing over 880 kg. Freech et al. [15] and Steffen et al. [16] simulated 400 & 44 kW APU systems respectively. The low NOx capability of the Micromix principle has already been successfully tested in a gas turbine APU GTCP 36-300[17].

Review of recent technical papers by leading researchers has led the authors choosing Brayton-Brayton hybrid cycle for detailed thermodynamic and emission analysis.

Though SOFC-APU system related studies are in progress but still it is not fully matured in terms of practical applications. Also, sizing and cost plays a vital role from design point of view and hence proposed model (Brayton-Brayton Hybrid cycle for APU) might be a fruitful candidate. The present paper carries out parametric analysis of Brayton-Brayton hybrid cycle for APU in terms of energy, exergy & emission performance.

MATERIALS AND METHODS

Thermodynamic analysis of the cycle had not been carried out earlier, hence in this work authors have attempted to fill up this research gap. The proposed configuration has various types of components whose parametric analysis is proposed to be done. The air after exiting the bottoming cycle compressor is passed through a gas to gas heat exchanger in order to increase its temperature with the help of energy/heat content of the topping cycle gas turbine exhaust. Hence in bottoming brayton cycle combustor has been substituted by a heat-exchanger. Heat-exchanger heats the bottoming brayton cycle compressor exit stream which in turn saves the fuel that would have to burnt otherwise. The proposed configuration consists of two brayton cycle and a heat-exchanger (figure 1).
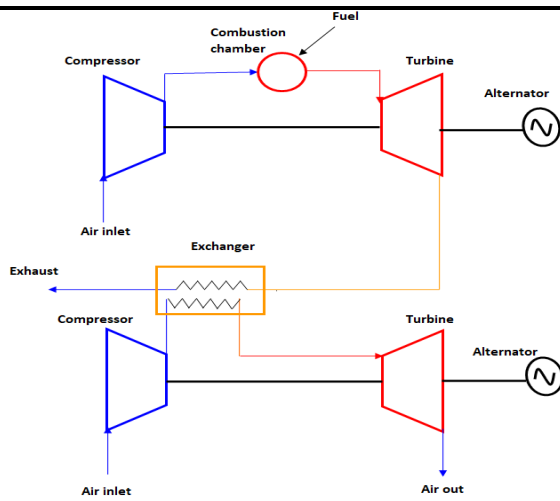
Fig. 1 Schematic representation of a Brayton-Brayton hybrid APU cycle

A. M*odeling of Components*

1. Air

Air is the working fluid of the cycle in the compressor. Various properties of air including c_p and enthalpy have been mathematically modeled as under:

The specific heat of air has been modeled based on polynomial given by Touloukian and Tadash Toulkinian and Tadash [17].

$$c_{pa} = 1.023204 - 1.76021 * 10^{-4}T + 4.0205 * 10^{-7}T^2 - 4.87272 * 10^{-11}T^3 \qquad (1)$$

The specific heat of gas has been modeled based on polynomial given by Touloukian and Tadash Toulkinian and Tadash [17].

$$c_{pg} = [15.276826 + 0.01005T - 3.19216 * 10^{-6}T^2 + 3.48619 * 10^{-10}T^3 + x_0(0.104826 + 5.54150 * 10^{-5}T - 1.67585 *$$

$$10^{-8}T^2 + 1.18266 * 10^{-12}T^3)]/V \qquad (2)$$

Thus, the enthalpy, entropy and exergy of the gas and air can be calculated as under:

$$h = \int_{T_a}^{T} c_p(T)\, dT \qquad (3)$$

$$\varphi = \int_{T_a}^{T} c_p(T)\, \frac{dT}{T} \qquad (4)$$

$$s = \varphi - Rln(\frac{p}{p_a}) \qquad (5)$$

$$B = h - T_a . s = h - T_a\varphi + RT_a ln(p - p_a) \qquad (6)$$

2. Compressor

Air is modeled to enter an axial flow compressor at ambient conditions. The temperature and pressure of air at the exit of compressor are calculated by the relation,

$$p_2 = p_1 * \pi_p \qquad (7)$$

$$\frac{T_2}{T_1} = \left(\frac{p_2}{p_1}\right)^{\frac{R}{\eta_{pc}*c_{pa}}} \qquad (8)$$

Compressor work and exergy destruction in compressor are determined by energy and exergy balance across the control volume of the compressor.

Compressor work is given by:

$$W_c = m_e h_e + \sum m_{cool,j} h_j \qquad (9)$$

The concept of polytropic efficiency (η_{pc}) has been used to account the thermodynamic losses within the compressor.

Exergy destruction in compressor has been calculated by the relation as under,

$$B_{d,c} = W_c + m_{c,in}\varepsilon_{c,in} - m_{c,e}\varepsilon_{c,e} \qquad (10)$$

3. Combustor modeling

The combustor has been modeled to experience a loss of 2% of the entry pressure at its exit. Natural gas has been modeled to burn in presence of excess air. The excess air used during combustion has about 1.5 times the required amount of air needed to

complete the stoichiometric reaction. The products of combustion at high temperature are led into the expansion turbine. Mass balance in combustion chamber is given by the relation:

$$m_3 = m_2 + m_f \qquad (11)$$

Energy balance in combustor has been given as under:

$$m_f . \Delta H_r . \eta_{comb} = m_3 h_3 - m_5 h_5 \qquad (12)$$

Mass of fuel required has been computed given by mass and energy balance of the combustor:-

$$m_{f} = \frac{[m_3 h_3 - m_5 h_5]}{[\eta_{comb} \Delta H_r - h_3]} \qquad (13)$$

The enthalpy of air exiting the combustor is given by: $h_3 =$

$$\frac{\left[\left\{15.276826(T_{RIT}-T_a)+0.01005\left(\frac{T_{RIT}^2-T_a^2}{2}\right)-3.1926*10^{-6}\left(\frac{T_{RIT}^3-T_a^3}{3}\right)+3.48619*10^{-10}\left(\frac{T_{RIT}^4-T_a^4}{4}\right)\right\}+x\{0.104826(T_{RIT}-T_a)+5.54150*10^{-5}\left(\frac{T_{RIT}^2-T_a^2}{2}\right)-1.67585*10^{-8}\left(\frac{T_{RIT}^3-T_a^3}{3}\right)+1.18266*10^{-12}(\frac{T_{RIT}^4-T_a^4}{4})\}\right]}{V} \qquad (14)$$

Exergy balance in combustor is given by the relation:-

$$B_{d,comb} = m_f \left[\Delta Gr + R_f T_a \ln\left(\frac{p_f}{p_a}\right)\right]_{comb} - (m_e \varepsilon_e - m_i \varepsilon_i)_{comb} \qquad (15)$$

4. Gas Turbine

The products of combustion exiting the combustor, enter the turbine rotor at a temperature being called here as turbine- inlet-temperature (TIT). High pressure and temperature gases expand sequentially in the expansion stages of axial flow turbine thus extracting the energy content in the gas. The blades of the turbine are modeled to be cooled using air film cooling technique discussed in author's previous work Sanjay et. al. [5].

$$\phi = \frac{m_{cool}}{m_g} = (1 - \eta_{iso,air}) \frac{St_{in} S_g}{\varepsilon_{cool}.t.cos\alpha} * \frac{c_{pg}(T_{g,in} - T_b)}{c_{p,cool}(T_b - T_{cool,in})} * F_{sa} \qquad (16)$$

The gas turbine blades of the bottoming cycle remain uncooled due to hot gas path temperature being lower than allowable blade temperature of 1123 K.

The pressure at the inlet of gas turbine is given as under:

$$p_3 = p_2 - (p_2 * 0.02) \qquad (17)$$

Gas turbine output and quantum of exergy destruction in gas turbine are computed from energy and exergy balance across the control volume of the gas turbine and are given by:

$$W_{gt} = m_{g,in}(h_{g.in} - h_{g,e}) + \sum m_{cool} (h_{cool,in} - h_{cool,e}) \qquad (18)$$

$$B_{d,gt} = (m_{g,in}\varepsilon_{g,in} - m_{g,e}\varepsilon_{g,e}) - W_{gt} \qquad (19)$$

B. Emission Analysis

The combustor of gas turbine has been modeled to burn natural gas having 86% CH_4 and 5% C_2H_6. There is a 2.5% drop in pressure of working fluid between the inlet and exit of the combustor. The flow in the combustor has been modeled to take place in three zones namely primary zone, intermediate zone and dilution zone. Maximum temperature is achieved in the primary zone, which gets reduced due to addition of secondary air to the main gas flow in the intermediate zone. The gas temperature is further reduced to manageable level in the dilution zone by mixing the main gas flow with secondary air. The gas turbine emission model has been adopted after refinement from the work of Rizk and Mongia [18]. The parameters controlling emission in the proposed model are taken to be equivalence ratio (ϕ), primary-zone-temperature, combustor inlet pressure and temperature and residence time. The emission of gas species namely NO_x, CO and UHC from the gas turbine that have been analyzed.

The parameters controlling emission from stationary gas turbines are as under:

1. **Equivalence Ratio (ϕ)** :- It represents the ratio of actual A/F ratio to the stoichiometric A/F ratio and is given as under:

$$\phi = \frac{(m_f/m_a)_{actual}}{(m_f/m_a)_{stoichiometric}} \qquad (20)$$

2. **Primary-Zone-Temperature (T_{PZ})**: - It represents the maximum temperature attained in the combustor and the combustor is generally designed to maximize this to attain superior thermodynamic performance of the gas turbine cycle. Primary-zone-temperature is given as [19]:-

$$T_{PZ} = A\sigma^\alpha \exp(\beta(\sigma + \lambda)^2) \left(\frac{p_3}{p_0}\right)^x \left(\frac{T_3}{T_0}\right)^y \left(\frac{H}{C}\right)^z \qquad (21)$$

where

$$\sigma = \phi \qquad \text{when } \phi \leq 1$$

$$\sigma = \phi - 0.7 \qquad \text{when } \phi \geq 1$$

$$\check{x} = a_1 + b_1\sigma + c_1\sigma^2$$

$$\check{y} = a_2 + b_2\sigma + c_2\sigma^2$$

$$\check{z} = a_3 + b_3\sigma + c_3\sigma^2$$

3. NO$_x$ Emission:- Oxides of nitrogen are generated due to oxidation of nitrogen at elevated temperatures within the combustor. Mass of NO$_x$ generated is also dependent upon residence time and equivalence ratio which is as under [18]:-

If $\phi \leq 1.08$

$$NO_x = 1E13(p_3 * 10^{-5}/1.4E6)^{aa}\exp(-71442/T_{pz})(7.56\phi^{-7.2} - 1.6)\tau^{0.64} \quad (22)$$

else,

$$NO_x = 1E13(p_3 * 10^{-5}/1.4E6)^{aa}\exp(-71442/T_{PZ})(5.21\phi^{-2.99} - 1.6)\tau^{0.64} \quad (23)$$

Where

$$aa = 11.949\exp(-\phi/5.76) - 10.0$$

4. CO emission:- Carbon-monoxide (CO) emission from gas turbine has been modeled to be dependent upon various parameters as under [18]:-

$$m_{co} = \exp\left(-\frac{CE}{T_{PZ}}\right) Cph \left(\frac{p_3 * 10^{-5}}{1.4E6}\right)^{a1} \left(\tau/0.5\right)^{a2} \qquad (24)$$

Where,

$$CE = 6.23E4\,\phi^{3.8}\exp((-\phi/0.56)^{1.75})$$

$$Cph = 4.54E3\phi^4 exp(-\phi/1.02)^{2.23}$$

$$a1 = -0.0447\phi^{-1.87} + 0.2$$

$$a2 = -0.362^{-1.9} + 0.2$$

5. UHC emission model:- Unburnt hydrocarbon emission from gas turbine combustor has been modeled to be mainly dependent on value of primary-zone-temperature attained in the combustor. Other parameters affecting UHC emission are residence time, combustor inlet pressure as well as pressure drop in combustor due excessive turbulence (induced in the combustor to enhance combustion). The mass of UHC emission has been detailed as under [18];

$$UHC = \frac{0.755E11\exp(9756/T_{PZ})}{(p_3 * 10^{-5})^{2.3}\tau^{0.1}(\triangle p_3/p_3)^{0.6}} \quad (25)$$

RESULTS AND DISCUSSION

The performance of the proposed cycle has been analyzed based on the mathematical modeling of cycle components as discussed in previous sections. A computer code in C++ language has been developed based on the mathematical modeling proposed earlier. Input data for the performance analysis has been listed in Table 1. The result has been validated with author previous work [7] and found within ±2% error. Based on the results obtained, graphs have been plotted and discussed.

Table 1: Input data for analysis for proposed Brayton-Brayton Cycle [5] [6] [7] [8] [9] [10] [20]
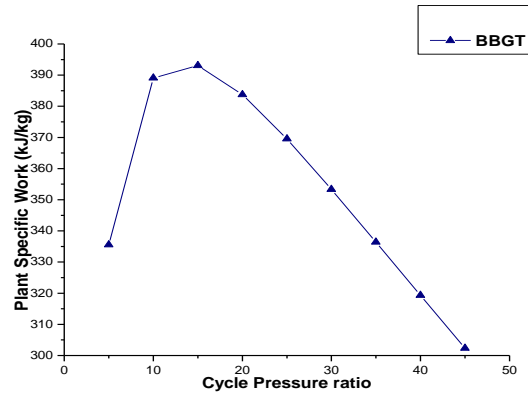

Figure 2. Effect of cycle pressure ratio on plant specific work for Brayton-Brayton cycle at TIT=1500 K
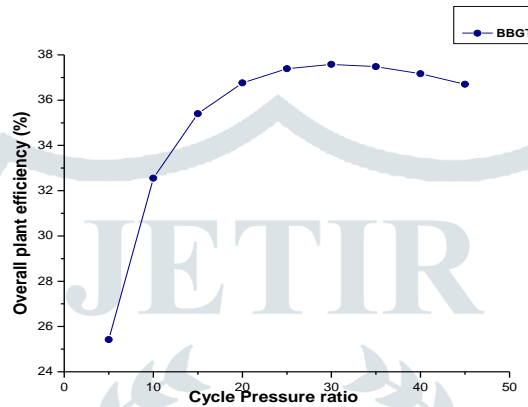

Figure 3. Effect of cycle pressure ratio on plant efficiency for brayton-brayton cycle at TIT=1500K

Figure 2 depicts the effect of cycle pressure ratio on plant specific work for a fixed value of Turbine-Inlet-Temperature of 1500 K. Result shows that plant specific work increases up to 393.07 kJ/kg at $r_{p,c}$ of 15 after this peak point it starts decreasing and reaches a minimum value of 302.33 at $r_{p,c}$ of 45. Hence the result shows the nature of curve is parabolic.

Figure 3 illustrates the effect of cycle pressure ratio on plant efficiency for a fixed value of Turbine-Inlet-Temperature of 1500 K. Result shows that the overall plant efficiency increases rapidly up to $r_{p,c}$ 20 and after this rate of increase of efficiency slows down reaches a maximum value of 37.58% at $r_{p,c}$ of 30. Hence figure shows that the plant efficiency increase with increase in cycle pressure ratio up to $r_{p,c}$ of 30 and after this it starts decreasing slowly and reaches a minimum value of 36.69 at $r_{p,c}$ of 45. This is due to parasitic compression work increasing steadily with increase in compression pressure ratio and thus effecting net gas turbine output which in turn affects overall plant performance.

| Component	Parameters
Gas property	$C_p = f(T)$ Enthalpy $h = \int C_p(T)\, dT$
Ambient condition	T_a=288K P_a=1.013 bar Relative humidity=60%
Inlet section	Δp_{loss}=1 percent of entry pressure
Compressor(Topping and bottoming cycle)	Isentropic efficiency (η_c)=86% Mechanical efficiency(η_m)=98%
Combustor	Δp_{loss}=2% of entry pressure η_{cc}=98%
Fuel	$C_{11}H_{21}$ $(LCV)_f$= 43370.596 kJ/kg Fuel inlet pressure = 110% of compressor exit pressure
Gas turbine(Topping and bottoming cycle)	Isentropic efficiency (η_t)=86% Mechanical efficiency(η_m)=98% Exhaust pressure=1.08 bar
Heat exchanger	Δp_{loss}=2% of entry pressure Effectiveness(ε_{rec})=92% Exhaust temperature for topping cycle=650K
Compressor(Bottoming cycle)	Pressure ratio=5
For Exergy analysis	TIT=1700K & Pressure ratio=25
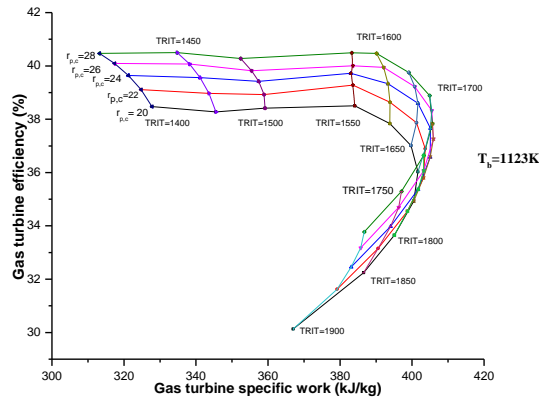
Figure 4: Variation of gas turbine efficiency and gas turbine specific work for different value of $r_{p,c}$ and TRIT in case of BGT

Figure 4 depicts the performance map showing the effect of *TRIT* and $r_{p,c}$ on gas turbine efficiency and specific work for BGT configuration at T_b=1123 K. At selected values of $r_{p,c}$, the gas turbine efficiency increases with *TRIT*, reaches a maximum value and then decreases. So, there is an optimum *TRIT* for every $r_{p,c}$ i.e., at $r_{p,c}$ =20, the optimum *TRIT* is at 1550K at which the gas turbine efficiency has been observed to be around 38.83% and specific work is approx. 383.84kJ/kg. Beyond this *TRIT*, the drop in gas turbine efficiency is very sharp. The prime reason that can be assigned to this behavior of the curve is that, at higher values of *TRIT*, the blade coolant flow rate becomes so high that it affects the gas turbine performance negatively. The maximum efficiency has been observed to be at $r_{p,c}$ =28 and *TRIT=1600K* at around 40.47%, whereas maximum specific work (405.91 kJ/kg) has been found to be at $r_{p,c}$ =26 and *TRIT*=1750K.
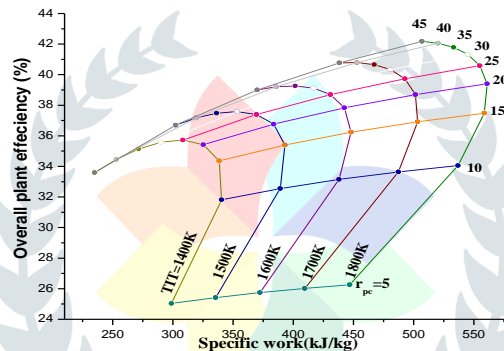

Figure 5: Influence of TIT and cycle pressure ratio on thermal efficiency, specific work Brayton -Brayton gas turbine cycle

Figure 5 demonstrates the performance map of brayton-brayton cycle illustrating the variation of specific work and plant efficiency for a different value of pressure ratio ($r_{p,c}$) and turbine inlet temperature (TIT). Result shows that for any value of TIT specific work increases upto $r_{p,c}$ 20 after this it specific work starts decresing. Also the plant efficiency for different value of TIT increases with increase in pressure ratio upto $r_{p,c}$=25 after this point it starts decreasing. Hence for different value of TIT both plant specific work and plant efficiency increases with increase in pressure ratio reaches a maximum value after that it starts decreasing. Overall plant efficiency and specific work increases with increase in TIT for different value of $r_{p,c}$ over the plotted range.

Figure 6 depicts histogram illustrating exergy performance of different components of proposed brayton-brayton cycle for a fixed value of $r_{p,c}$=25 and TIT=1700K. Result shows that gas turbine of the topping cycle has the rational efficiency of about 37.26%, whereas 1.53% for bottoming cycle. This is because TIT of bottoming cycle is constrained by turbine exhaust temperature of topping cycle. Combustion chamber exhibits highest value of exergy loss of about 28%. Overall stack exhaust gas exergy loss is about 15% and unaccounted exergy loss is about 8.25%.
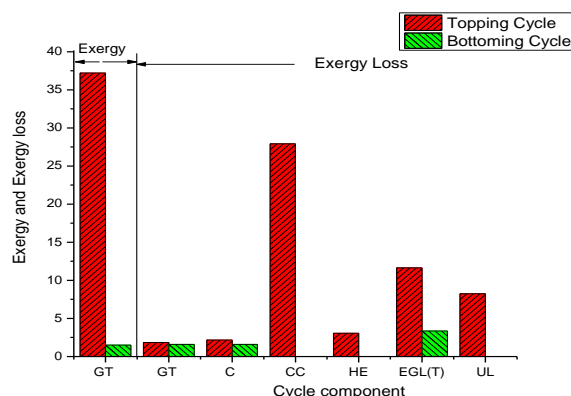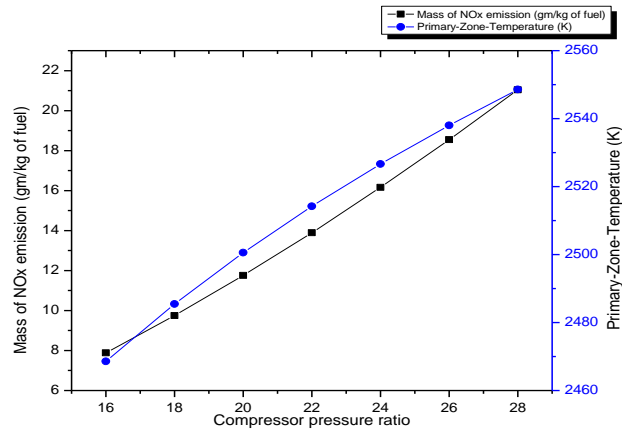

Figure 6: Component wise Exergy and Exergy loss

Figure 7: Variation of NOx emission and Primary-Zone-Temperature With Compressor pressure Ratio

Figure 7 depicts the nature of variation of NO_X emission and primary-zone-temperature for the proposed cycle with increase in operating parameter $r_{p,c}$. The graph shows that with increase in compressor pressure ratio there is increase in NO_X emission as well as primary-zone-temperature. NO_X emission varies almost linearly with a slight curvature in the mid compressor pressure ratio range between $r_{p,c}$ =21 to $r_{p,c}$ =23. The behavior is to the fact that at higher $r_{p,c}$, the average temperature inside the combustor increases due to increased combustor inlet air temperature and hence higher T_{pz}. NO_X emission for the proposed cycle with a gas turbine having a compressor pressure ratio of 22 is around 13.89 g/kg of fuel.
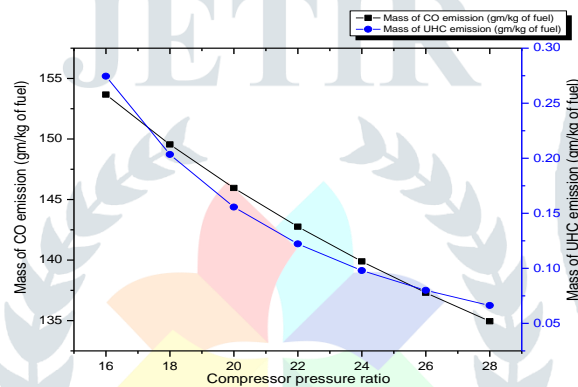

Figure 8: Variation of CO and UHC emission With Compressor pressure Ratio

Figure 8 illustrates the nature of variation of CO and UHC emission for the proposed cycle with operating parameter $r_{p,c}$. The graph shows that with increase in compressor pressure ratio there is decrease in NO_X emission as well as primary-zone-temperature. UHC emission varies almost linearly with a slight curvature in the mid compressor pressure ratio range between $r_{p,c}$ =21 to $r_{p,c}$ =23. The behavior is due to the fact that at higher $r_{p,c}$, the average temperature inside the combustor increases due to increased combustor inlet air temperature and hence higher T_{pz}.
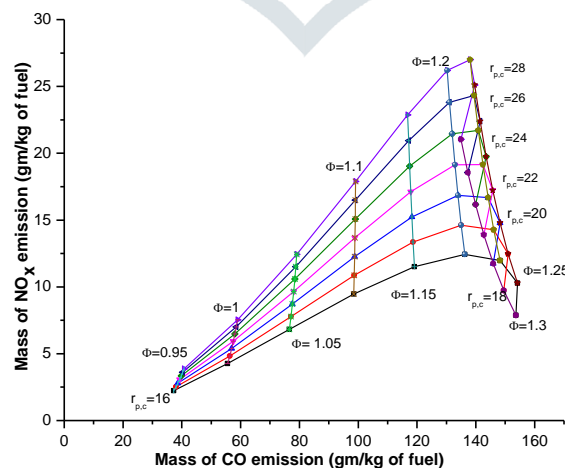

Figure 9: Emission performance map for Brayton-Brayton gas turbine cycle

Figure 9 shows an emission performance map illustrating the variation of the NO_x emission for Brayton-Brayton gas turbine cycle for different compressor pressure ratio ($r_{p,c}$) and equivalence ratio(Φ). The performance map shows that for a chosen value of $r_{p,c}$, on increasing the value of equivalence ratio, NO_x emission initially increases, reaches a maximum value at Φ =1.2 then starts decreasing. This is mostly due to the higher value of primary-zone-temperature at Φ =1.2.

CO emission has been observed to increase at a variable rate with an increase in equivalence ratio. The rate of increase has been observed to be almost constant upto $\Phi=1.2$, where after on increasing equivalence ratio, the rate of increase in CO emission decreases due lower values of primary-zone-temperature which leads to lower level of complete combustion.

CONCLUSION

The thermodynamic emission analysis of proposed hybrid cycle has been carried out. Based on the results following conclusion have been made:

1) Brayton-brayton cycle provides the maximum available energy (about 40%)

2) Brayton-brayton cycle gives maximum work output between 450-550 kJ/kg.

3) Exergy loss in combustor is approximate 29% which is maximum.

4) Mass of NO_X emission is increases with compressor pressure ratio whereas mass of CO emission decreases with increase in compressor pressure ratio.

5) Primary-Zone-Temperature increases with increase in compressor pressure ratio.

6) UHC emission decreases with increase in compressor pressure ratio.

REFERENCES

[1] Wu, S. Li, Y. 2014 Fuel Cell Applications On More Electrical Aircraft. 17th int. Conf. Electr. Mach. Syst. IEEE; 2014. p. 198-201. https://doi.org/10.1109/ ICEMS.2014.7013481.

[2] Sarlioglu, B. Morris, CT. 2015 More Electric Aircraft: Review, Challenges, and Opportunities for Commercial Transport Aircraft. IEEE Trans. Transp. Electrif. 154-64. https://doi.org/10.1109/TTE.2015.2426499.

Masiol, M. Harrison. RM. 2014 Aircraft Engine Exhaust Emissions and Other Airportrelated Contributions to Ambient Air Pollution: A Review. Atmos Environ, 95 pp 409-55. https://doi.org/10.1016/j.atmosenv.2014.05.070.

[3] Braun RJ, Gummalla M, Yamanis J. 2009 System Architectures For Solid Oxide Fuel Cell-Based Auxiliary Power Units In Future Commercial Aircraft Applications, J Fuel Cell Sci Technol https://doi.org/10.1115/1.3008037.

Sanjay, Singh, O. Prasad B.N. 2008 Influence of different means of turbine blade cooling on the thermodynamic performance of combined cycle, Applied Thermal Engineering. 28 pp 2315–2326.

[4] Sanjay 2011 Investigation of effect of variation of cycle parameters on thermodynamic performance of gas-steam combined cycle, Energy. 36 pp 157-67

Kumari, A. Sanjay 2015 Investigations of parameters affecting exergy and emission performance of basic and intercooled gas turbine cycles, Energy. 90 pp 525-536

[5] Mishra, S, Sanjay, 2018 Energy and Exergy Analysis of Air-Film Cooled Gas Turbine Cycle: Effect of Radiative heat transfer on blade coolant requirements, Applied Thermal Engineering, 129 pp 1403-1413.

Shukla, AK. Singh, O. 2016 Performance evaluation of steam injected gas turbine based power plant with inlet evaporative cooling, Applied Thermal Engineering. 102 pp 454–464

Mishra, S. Sohret, Y. Sanjay, 2018 Advanced Exergy Analysis of Air-Film Blade Cooled Marine Gas Turbine (LM2500+), SAE Technical Paper 2018-01-1372 doi: 10.4271/2018-01-1372.

[6] Choudhary, T. Sahu, MK, Krishna, S. 2017 Thermodynamic Analysis of Solid Oxide fuel cell gas Turbine hybrid System for Aircraft Power Generation, SAE Technical paper https://doi.org/10.4271/2017-01-2062.

[7] Freeh, JE, Pratt, JE. And Brouwer, J. 2004; Development of a Solid-Oxide Fuel Cell/Gas Turbine Hybrid System Model for Aerospace Applications," Proceedings of ASME Turbo Expo, 2004, doi:10.1115/GT2004-53616

[8] Chakravarthula, VA and Roberts, R.A. 2017 Transient Analysis of an Innovative Cycle Integrating a SOFC and a Turbogenerator for Electric Propulsion, Proceedings of ASME Turbo Expo, doi:10.1115/GT2017-64804.

Rajashekara, K. 2005 Hybrid Fuel-Cell Strategies for Clean Power Generation IEEE Transactions on Industry Applications 41 (3) pp 682-689 doi:10.1109/IAS.2004.1348753

Freeh, J.E., Steffen, C.J., and Larosiliere, L.M., 2005 Off-Design Performance Analysis of a Solid-Oxide Fuel Cell/Gas Turbine Hybrid for Auxiliary Aerospace Power, ASME 23rd International Conference on Fuel Cell Science, Engineering and Technology, doi:10.1115/FUELCELL2005-74099.

Steffen, C.J., Freeh, JE, and Larosiliere, L.M. 2005 Solid Oxide Fuel Cell/Gas Turbine Hybrid Cycle Technology for Auxiliary Aerospace Power, Proceedings of ASME Turbo Expo, 2005, doi:10.1115/GT2005-68619.

Funke H. H.-W., Boerner S, Hendrick P, Recker E, Elsing R. Development and integration of a scalable low NOx combustion chamber for a hydrogen fuelled aero gas turbine, Progress in propulsion physics vol. 4, 2013

[9] Touloukain, YS, Tadash, M. 1970 Thermo-physical properties of matter, In the TPRC Data Series, vol. 6. New York, Washington: IFI/PLENUNM; 1970.

Rizk, NK. & Mongia, HC. 1993 Semi analytical Correlations for NOx, CO, and UHC Emissions. J Eng. Gas Turbine Power Vol. 115 3.

[10] Gulder, OL. 1986 Flame Temperature Estimation of Conventional and Future Jet Fuels. Transaction of the ASME, Vol. 108.

[11] Y. Sohret, E. Açıkkalp, A. Hepbasli, T. H. Karakoc, Advanced exergy analysis of an aircraft gas turbine engine: Splitting exergy destructions into parts, Energy. (2015) 1219-1228.